[7] Monkewitz, P.A., Feedback control of global oscillations in fluid systems, AIAA Paper 89-0991, 1989.
[8] Morkovin, M.V. and Reshotko, E., Dialogue on progress and issues in stability and transition research, in *Laminar-Turbulent Transition*, Arnal, D. and Michel, R., Eds., Springer-Verlag, Heidelburg, 1990.

13.4 Coherent Structures

David G. Bogard and Karen A. Thole

Introduction

The term "coherent structures" refers to a wide variety of spatially coherent events that have been identified in turbulent flows using flow visualization or analysis of velocity or temperature fields measured experimentally or numerically simulated. Descriptions of coherent structures range from rather loosely defined "turbulent bulges," which occur in the outer region of wall bounded turbulence, to specific velocity field characteristics such as large turbulent shear stress or velocity gradients. Interest in coherent structures was stimulated by a number of flow visualization studies in the 1960s that showed spatially coherent elements of fluid which appeared to be important in turbulent transport processes. Later, quantitative studies were conducted using conditional sampling (described later in this section) to educe the average velocity characteristics. Coherent structures are generally identified in terms of a velocity "signature." The weakness in these experimental studies was establishing the relationship between the point measurement of particular velocity characteristics or signatures to the spatially coherent events observed by flow visualization. More recently, direct numerical simulation of the turbulent flow fields have enabled studies of the full three-dimensional characteristics of the coherent structures. The following is a discussion of a number of the more thoroughly studied coherent structures in wall bounded and free shear flows.

Coherent Structures in Wall Bounded Turbulence

An important motivation for studying coherent structures is their importance in generating turbulence shear stress. As discussed in Section 13.5 for turbulent wall flows, increased momentum transport due to turbulence and turbulence energy production occur due to the turbulence shear stress, $-\rho\overline{u'v'}$. For turbulent wall flows the $u'v'$ product tends to occur intermittently with sharp spikes that are predominantly negative, as shown in Fig. 13.14. Although the average value of the correlation coefficient is $\overline{u'v'}/u'_{rms}v'_{rms} = -0.45$, the instantaneous spikes are often 10 to 20 times greater than this, and these negative spikes are the major source of turbulent shear stress. The study of coherent structures provides a means of understanding what flow mechanisms cause these intermittent spikes of $u'v'$, and hence turbulent transport and production of turbulence energy.

Near-Wall Structure

Immediately adjacent to the wall, within the viscous sublayer, the velocity field is quite nonuniform with narrow, long regions of low velocity and relatively shorter regions of high velocity. When dye is introduced through a slit in the wall, the dye accumulates into the long low velocity regions and the near wall region has a "streaky" appearance. These low velocity streaks have also been visualized with hydrogen bubble time lines which directly show the low velocity and high velocity regions. Streaks are generally aligned with the direction of flow, although they follow a somewhat meandering path. The average streak spacing of $\lambda^+ = 100$ ("+" indicates nondimensionalization with viscous variables ν and u_τ) is well established, but the range of momentum thickness Reynolds numbers for these studies is limited

$u'v'/u$

FIGURE 13.14 Typica

to $Re_\theta < 6000$ [28]. Generally, the width c individual streaks ma lengths [17].

The flow mechanis shear layers around th to evolve into vortice streaks are commonl at the wall into longi on a numerical simu vortical structures do counter-rotating pair

Coherent structure are bursts and sweep sweeps involve wallw visualization studies When the dye slit tec observed to intermitt single ejection or seve a single streak are kn suspended particles i that moves toward t the instantaneous tu average [16].

Quantitative

Many quantitat was identified using bursts and sweeps [3C in one of four quadr u' velocity is negative

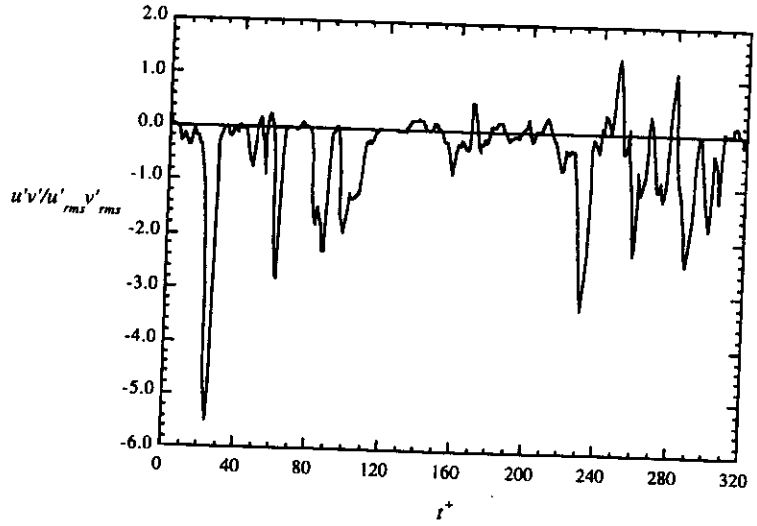

FIGURE 13.14 Typical time record of the $u'v'$ product for a turbulent boundary layer at $y^+ = 15$.

to $Re_\theta < 6000$ [28]. Individual streak spacing is quite variable ranging from $\lambda^+ = 20$ to $\lambda^+ = 250$. Generally, the width of the low speed region is relatively narrow, less than 20 viscous lengths (ν/u_τ), but individual streaks may be as wide as 60 viscous lengths. Streaks can extend for more than 1000 viscous lengths [17].

The flow mechanisms responsible for the formation of streaks are of prime interest because the sharp shear layers around the low speed streaks. These shear layers are the origin of instabilities that are thought to evolve into vortices that subsequently induce the ejections and sweeps as discussed below. Although streaks are commonly thought to occur by the action of streamwise vortices sweeping low velocity fluid at the wall into longitudinal structures, experimental evidence of this is not conclusive. Recent analysis on a numerical simulation of a turbulent boundary layer flow [25] showed that although streamwise vortical structures do occur adjacent to streaks, they were generally single vortex structures rather than counter-rotating pairs, and they were relatively short rather than existing along the full length of the streak.

Coherent structures that are directly associated with producing large $-\rho\overline{u'v'}$ turbulent shear stresses are bursts and sweeps. Bursts involve the ejection of low velocity fluid away from the wall region, and sweeps involve wallward directed high velocity fluid. Both of these structures were first defined in flow visualization studies [20, 24], and were later studied quantitatively using velocity probe measurements. When the dye slit technique is used to visualize streaks as described above, the dyed low-speed streak is observed to intermittently lift away from the wall and eject outwards. A single streak may be the source of a single ejection or several ejections that are grouped together. Single ejections, or groups of ejections from a single streak are known as bursts. Sweeps, visualized with hydrogen bubble time lines or by tracking suspended particles in the flow, originate from about $y^+ = 30$ to 100 and are relatively high-speed fluid that moves toward the wall. By quantitatively analyzing flow visualization records, it was found that the instantaneous turbulent shear stress during bursts and sweeps is many times larger than the time average [16].

Quantitative Measurements of Near-Wall Structures

Many quantitative studies of bursts and sweeps have been completed in which the burst and/or sweep was identified using a particular velocity signature. A quadrant technique was proposed for identifying bursts and sweeps [30, 32]. In the quadrant technique the instantaneous $u'v'$ product is classified as being in one of four quadrants depending on the sign of u' and v'. Quadrant 2 (Q2) events occur when the u' velocity is negative, i.e., lower than the mean, and vertical velocity is positive, i.e., away from the wall;

consequently Q2 events were associated with bursts. Similarly, quadrant 4 (Q4) events are wall-ward directed, high velocity events and are associated with sweeps. A direct comparison of the visualized bursts and Q2 events showed a good correspondence between the ejections within a burst and Q2 events which have a $u'v'$ magnitude above a given threshold [6]. Consequently, the quadrant technique is generally considered to be a reliable means for identifying ejections. Furthermore, groups of closely spaced ejections, found with this technique, constituted a single burst event [6]. A similar confirmation of the quadrant technique for identifying sweeps has not been done; however, in many cases the sweep has been defined as a Q4 event with $u'v'$ magnitude above a reasonable threshold level. Note also that the validation of the quadrant technique was done using measurements close to the wall ($y^+ = 15$). Quadrant detections at larger distances from the wall would be less correlated with bursts as defined from the flow visualization perspective.

The velocity fields within and surrounding ejections and sweeps have been measured using a technique known as conditional sampling. In this technique the time record of some flow variable (generally the velocity) is sampled during a short period before and after a prescribed condition occurs, such as an ejection or a sweep. A mean velocity pattern is then obtained by averaging a large ensemble of these samples. Conditional sampling using quadrant detection has been used by Gan [14] to reconstruct the three-dimensional average flow patterns associated with bursts and sweeps. Defect velocity contours in the vertical-streamwise plane are presented in Fig. 13.15 for the primary ejection within a burst detected at $y^+ = 30$. The defect velocity associated with the ejection has an elongated shape with a sloped back across

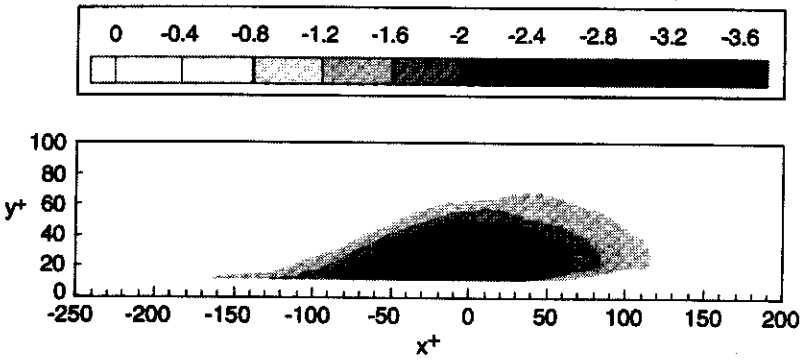

FIGURE 13.15 Ensemble average of the u'-velocity for the primary ejection in bursts conditionally sampled at $y^+ = 30$ using quadrant 2 detection.

which there is a large velocity gradient, especially toward the top of the ejection. This large velocity gradient is due to a shear layer caused by the impact of high velocity fluid on the back of the low velocity fluid as it moves away from the wall. Note that the maximum defect velocity occurring at a height of $y^+ = 30$ is a consequence of this being the detection height. Cross sections of the velocity fields associated with the primary ejection within a burst are presented as a time sequence in Fig. 13.16 showing an upward velocity with a maximum magnitude of $1.4u_\tau$ and extending to $y^+ = 80$. Also evident is a strong spanwise velocity along the wall toward the center of the ejection, which is consistent with the concept of streamwise vortices stimulating the ejection. Note that velocity measurements were made only on one side of the detector probe because ensemble averaging will necessarily result in a symmetric structure about the detection point, even if individual events are not symmetric.

Conditional sampling analysis of the sweep structure shows a region of increased streamwise velocity similar in size to that found for ejections. Cross sections of the velocity field associated with a sweep, shown as a time sequence in Fig. 13.17, show a strong wallward-directed velocity extending from beyond

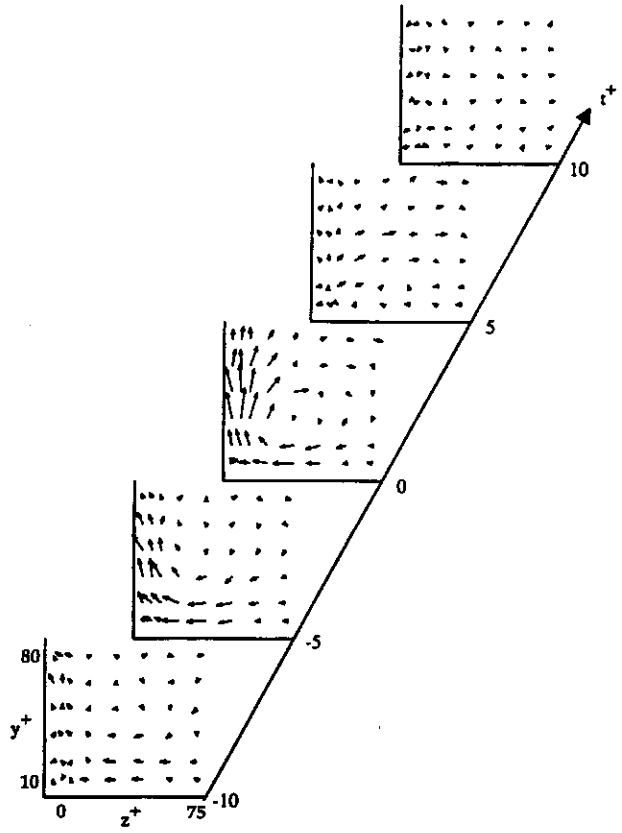

FIGURE 13.16 Time sequence of the ensemble average of the $v' - w'$ velocity vectors for the primary ejection in bursts conditionally sampled at $t^+ = 0$, $z^+ = 0$, and $y^+ = 30$ using quadrant 2 detection.

$y^+ = 80$ to below $y^+ = 20$, but diminishing considerably by $y^+ = 10$. Spanwise flow along the wall emanates from the center of the sweep. A strong spanwise flow occurs prior to the sweep detection that may be due to the leading edge of the sweep interacting with the wall and being diverted laterally. For both ejections and sweeps the duration of the strong upflow and downflow, respectively, is $\Delta t^+ = 5$ to 10. One should recognize that this duration corresponds to time needed to traverse through the probe position and is indicative of the streamwise length of the ejection or sweep, not the lifetime of the event. A final note of caution, it is important to recognize that the velocity field obtained in this manner represents the average velocity field of a large number of events (over 300 were used to obtain the velocity fields described above), and that individual events can be very different than this average event.

Interactions between elements of high speed and low speed fluid result in distinct regions of high shear. These shear layers are often identified from measurements of the u' velocity component using the VITA detection algorithm. Originally, the VITA technique was developed to identify periods of large variance in the velocity signal that were postulated to be associated with bursts [4]. However, because the u' variance is obtained over a relatively short averaging time, the VITA technique actually identifies large gradients in the velocity signal. These gradients, which are generally classified as either positive or negative, are due to sharp shear layers in the flow. Although positive shear layers occur with bursts as high velocity fluid impacts low velocity fluid ejecting away from the wall, VITA events are not exclusively associated with bursts.

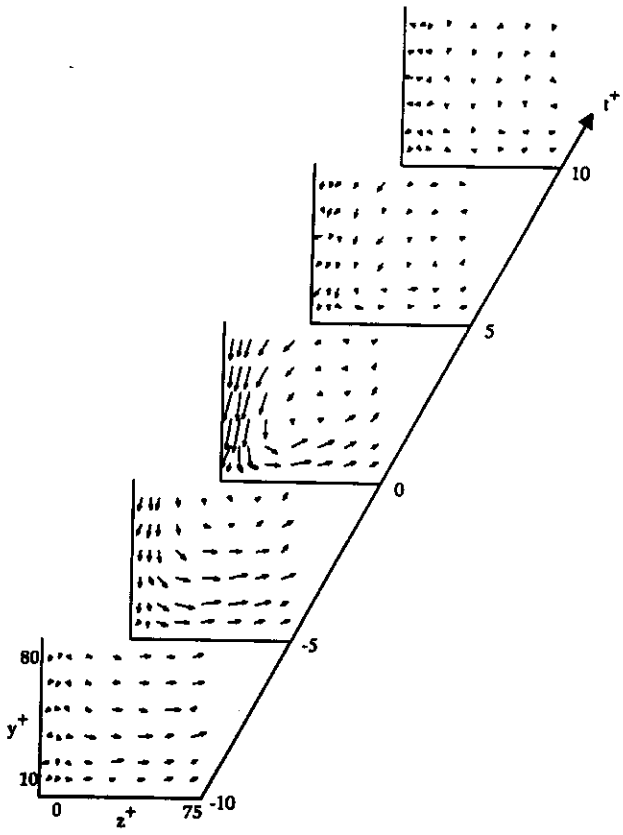

FIGURE 13.17 Time sequence of the ensemble average of the $v' - w'$ velocity vectors for the primary $u'v'$ spike in sweeps conditionally sampled at $t^+ = 0$, $z^+ = 0$, and $y^+ = 30$ using quadrant 4 detection.

A Physical Model for Bursts and Sweeps

The preceding descriptions of the velocity fields associated with bursts and sweeps do not indicate the processes which cause the uplifting of low speed fluid in the case of bursts, nor the wallward-directed motion for sweeps. Some understanding of the flow mechanisms comes from observations in many flow visualization studies that distinct vortices, either transverse vortices or streamwise vortices, are commonly associated with bursts and sweeps. Many conceptual models of physical mechanisms generating bursts and sweeps have been proposed, and every one of these models incorporates some kind of vortical structure. A number of these conceptual models hypothesize that the central element is a horseshoe or hairpin-shaped vortical structure with two legs that are oriented quasi-streamwise, extend away from the wall, and then connect to an overlying transverse vortex. Direct experimental verification of this type of vortical structure has not been possible because whole-field, time-resolved velocity measurements would be required.

More recently, direct Navier–Stokes numerical solutions of turbulent wall flows have been developed to provide simulated wall turbulence data bases that can be analyzed to determine the role of various vortical structures in burst and sweep generation. Robinson, Kline, and Spalart [27] and Robinson [25, 26] completed a detailed analysis of a simulated turbulent boundary data base. This turbulent boundary layer simulation, obtained computationally by Spalart [29], had velocity field statistics which compared well with experiments, and the coherent structures appeared similar to flow visualization studies. However, the momentum thickness Reynolds number of $\mathrm{Re}_\theta = 670$ and the friction velocity Reynolds number of $\mathrm{Re}^* = \delta u_\tau/\nu = 350$ were small. Near-wall structures are probably well represented in this simulation, but

differences between inner and outer structures are not well resolved because of the low Reynolds number. A major part of these studies was to determine the correlation between various coherent structures, particularly the bursts and sweeps described above, and vortical structures that might induce the burst or sweep motions. Identifying vortical structures is not a straightforward process, and Robinson [25] evaluated several different procedures before concluding that the vortical structures are best identified by low pressure regions in the interior of the vortices. Kasagi et al. [19] also concluded that there is good correspondence between the core of vortices and low pressure regions. From his analysis of the simulation data base, Robinson [26] observed that there were a wide variety of vortical structures, but distinct hairpin or horseshoe vortical structures were relatively rare. Most of the vortical structures were classified as arches or quasi-streamwise. The arch like vortical structures were basically transverse vortices with one end, or both ends, curled down toward the wall. The quasi-streamwise vortical structures were primarily single structures rather than counter-rotating pairs, and were oriented primarily in the streamwise direction, but angled away from the wall and skewed in the spanwise direction. Transverse vortices were found to dominate in the outer part of the boundary layer, and quasi-streamwise vortices were found to dominate in the near wall region.

Robinson's [26] study showed that most bursts and sweeps occurred in association with the arch-like and quasi-streamwise vortices as indicated in the schematic shown in Fig. 13.18. Near the wall, most bursts and sweeps occurred along the side of a quasi-streamwise vortex element either as single bursts, or sweeps, or as a burst and sweep pair. Further from the wall many Q2 events occurred on the upstream side of an arch vortex, and Q4 events occurred along the side of the arch (in the outer region these Q2 and Q4 events are not necessarily bursts or sweeps, respectively).

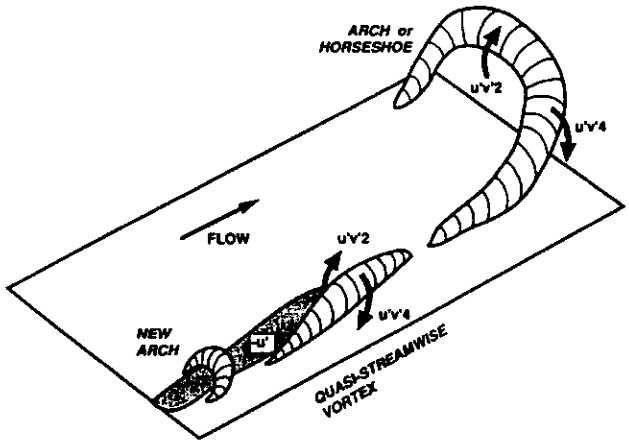

FIGURE 13.18 Generalized physical model of the arch or horseshoe vortex and quasi-streamwise vortex slowing the generation of ejections ($u'v'2$) and sweeps ($u'v'4$) by these structures [25].

Given that bursts and sweeps are associated with quasi-streamwise vortices near the wall, the origins of these vortices has been investigated in several recent studies using analysis of numerical simulations of channel flow [7, 3, 23]. Each of these simulations was at relatively low Reynolds numbers of $Re^* = (h/2)u_\tau/\nu = 125$ to 150, considerably lower than the boundary layer simulation analyzed by Robinson [26], so there is some question as to the generality of the results. The consensus conclusion from these studies was that the quasi-streamwise vortices evolve from a regenerative process in which an existing quasi-streamwise vortex, denoted as a "parent vortex", induces a new counter-rotating vortex. Brooke and Hanratty [7] found that the new quasi-streamwise vortex originated at the wall when the downstream part

of the parent vortex moved away from the wall and induced a spanwise flow between the parent vortex and the wall. Furthermore, all three studies found that tilting of vertically oriented vorticity was a major contributor to the development of new quasi-streamwise vortices.

Outer Structure

Bursts, sweeps, and streaks are coherent structures that occur in the near-wall region, i.e., $y^+ < 100$. Large-scale coherent structures that extend across the boundary layer are also clearly evident from flow visualization studies and multi-probe measurements. Flow visualizations in boundary layer flows show bulges of turbulent motions separated by narrow regions of nonturbulent flow; hence the name "turbulent bulges" or "large-scale motions." These large-scale structures were also evident from the velocity space–time correlation measurements of Favre et al. [12] and Kovasznay et al. [21], which showed significant correlations of the velocity field extending across the boundary layer height. Inclined temperature "fronts" across the boundary layer height, associated with the back edge of large-scale structures, were identified by an array of temperature sensors by Chen and Blackwelder [10]. These structures span the boundary layer height from δ to 2δ. Different investigations have found that the structures are inclined downstream at angles ranging from 10° to 45°. Many of these studies have indicated a correlation between these large-scale motions and near wall bursts and sweeps. Although there is little doubt that the large-scale motions have some effect on near-wall bursts and sweeps, whether or not this is a major effect is an unresolved issue.

Effect of Drag Reduction Techniques on Coherent Structures

An insight into the physical characteristics of turbulent wall flows is given by the effects of various drag reduction techniques on coherent structures. The most effective drag reduction technique is the introduction of dilute polymer solutions into the near wall region. With very small concentrations of polymers, drag reductions as much as 70% can be achieved. This drag reduction occurs because the long chain of polymer molecules impede the turbulent motions, resulting in an increase in the streak spacing (as much as doubled) and a similar decrease in the burst frequency. However, the polymer solutions were found to be effective only when the polymer was in the buffer region; polymer in the viscous sublayer or in the outer part of the flow had no effect on the coherent structures and no drag reduction. There are two important implications from these results. First, the streak structure, particularly the streak spacing, is a consequence of some overlying structure in the buffer region, i.e., essentially the streaks are a passive indication of these overlying structures. Second, structures near the wall are the critical mechanisms for turbulence production, and suppression of these structures can dramatically reduce turbulence levels independent of the outer layer.

Another drag reduction technique that has been extensively studied is the large eddy break-up (LEBU) device. For this technique, thin plates are positioned in the outer part of the boundary layer and parallel with the wall. Plate widths of about the boundary layer thickness are used, and typically two plates spaced several boundary layer thicknesses apart are used. The concept behind this technique is to suppress, or "break up," the large scale motions. At a short distance downstream of the LEBU the wall shear and ejection frequency are reduced as much as 20%, but rise again to normal levels farther downstream [5]. This result is important in showing that the outer region is not totally passive, although the effect on reducing drag is not as strong as when the near wall structure is suppressed.

A reduction in wall shear can also be induced by riblets on the wall. Riblets are very small ridges protruding from the wall and aligned parallel with the flow. With a spacing and riblet height of nominally 20 wall units, Walsh [31] showed a maximum drag reduction of about 5%. The precise mechanism of drag reduction with riblets has not been established, but the low drag reduction obtained with riblets is further evidence that turbulent structures away from the wall, i.e., in the buffer region, are the critical structures in producing turbulence.

Coherent Structures in Free Shear Flows

Large-scale coherent structures are readily apparent in many free shear flows. In the wake of bluff bodies there is a shedding of a regular train of eddies, the Kármán vortex street. For mixing layers between two co-flowing streams or for free jets, a systematic array of vortices is generated by the Kelvin–Helmholtz instability mechanism in the shear layer. These coherent structures are fundamentally different than the wall-bounded coherent structures discussed previously in that they are not produced by the turbulence, but by the instability of the shear layer. Consequently, these coherent structures are evident in laminar, transitional, and turbulent shear layers. Extensive studies of these coherent structures have been motivated by the recognition of the importance of these structures in the growth of the shear layers, production of turbulence, and as a means of controlling shear layer growth and turbulent mixing.

For turbulent plane mixing layers, growth of the shear layer and turbulent mixing are strongly influenced by vortex pairing [8, 9]. Vortex pairing occurs when two vortices in the train of two-dimensional spanwise vortices generated by the shear layer interact with one vortex structure rotating about the other, resulting in an amalgamation of the two vortices into a single vortex. A similar vortex pairing occurs for axisymmetric jet flows that have large-scale vortices that can have either axisymmetric ring vortices, or spiral vortices, or a transitional state between the two modes [11]. Because of the importance of vortex pairing in the development of mixing layers and axisymmetric jets, effective control of the growth and mixing can be achieved by stimulating or "forcing" the generation of vortices at specific frequencies. This forcing can be achieved by introducing small perturbations to the flow at the initial stages that stimulate the instability leading to the roll up of the vortices. By forcing the generation of vortices at the appropriate frequency and phase, the growth of the mixing layer or axisymmetric jet can be increased or decreased relative to the natural state [22].

Between the primary large-scale two-dimensional spanwise vortices in mixing layers there exists smaller scale coherent structures in the form of an array of streamwise, counter rotating vortices [2]. These streamwise vortices, sometimes known as ribs, are three-dimensional instability structures that are highly sensitive to initial disturbances in the mixing layer. Induced velocities by the counter-rotating vortices direct fluid into and out of the primary vortices.

For turbulent wakes behind cylinders, Kármán vortices are the dominant coherent structures in the near to intermediate distances downstream. Turbulent shear stresses are maximum between the vortices which Hussain [18] interpreted as an indication of rib-like streamwise vortical structures similar to those observed in mixing layers. Far downstream, several studies indicate a large scale "double roller" three-dimensional structure [1, 13, 15]. These structures are not readily apparent, and have been identified by sophisticated measurement and analysis. The counter-rotating double roller vortex tubes are side by side in the spanwise direction with their axes of rotation inclined in the streamwise direction, parallel to the mean rate of strain. These structures are thought to be important contributors to turbulent stresses and entrainment.

References

[1] Antonia, R.A., Browne, L.W.B., Bisset, D.K., and Fulachier, L., A description of the organized motion in the turbulent wake of a cylinder at low Reynolds number, *J. Fluid Mech.*, 184, 423–444, 1987.

[2] Bernal, L.P. and Roshko, A., Streamwise vortex structure in plane mixing layers, *J. Fluid Mech.*, 170, 499–525, 1986.

[3] Bernard, P.S., Thomas, J.M., and Handler, R.A., Vortex dynamics and the production of Reynolds stress, *J. Fluid Mechanics*, 253, 385–419, 1993.

[4] Blackwelder, R.F. and Kaplan, R.E., On the wall structure of the turbulent boundary layer, *J. Fluid Mech.*, 76(1), 89–112, 1976.

[5] Bogard, D.G. and Coughran, M.T., Bursts and ejections in a LEBU-Modified Boundary Layer, *Sixth Symp. Turbulent Shear Flows,* Toulouse, France, 1987.

[6] Bogard, D.G. and Tiederman, W.G., Burst detection with single-point velocity measurements, *J. Fluid Mech.,* 162, 389–413, 1986.

[7] Brooke, J.W. and Hanratty, T.J., Origin of turbulence-producing eddies in a channel flow, *Phys. Fluids A,* 5(4), 1011–1022, 1993.

[8] Browand, F.K. and Weidman, P.D., Large scales in the developing mixing layer, *J. Fluid Mech.,* 158, 127–144, 1976.

[9] Brown, G.L. and Roshko, A., On density effects and large structure in turbulent mixing layers, *J. Fluid Mech.,* 64, 775–816, 1974.

[10] Chen, C.H.P. and Blackwelder, R.F., Large-scale motion in a turbulent boundary layer: A study using temperature contamination, *J. Fluid Mech.,* 89, 1–31, 1978.

[11] Dimotakis P.E., Miake-Lye, R.C. and Papantoniou, D.A., Structure and dynamics of round turbulent jets, *Phys. Fluids,* 26, 3185–3191, 1983.

[12] Favre, A.J., Gaviglio, J.J., and Dumas, R., Space-time double correlations and spectra in a turbulent boundary layer, *J. Fluid Mech.,* 2, 313–341. 1957.

[13] Ferre, J.A., Mumford, J.C., Savill, A.M., and Giralt, F., Three-dimensional large-eddy motions and fine-scale activity in a plane turbulent wake, *J. Fluid Mech.,* 210, 371–414, 1957.

[14] Gan, C.L., Spatial characteristics of near wall turbulence-generating events in natural and perturbed turbulent boundary layers, Ph.D. dissertation, University of Texas at Austin, 1994.

[15] Giralt, F. and Ferre, J.A., Structure and flow patterns in turbulent wakes, *Phys. Fluids,* 5(7), 1783–1789, 1993.

[16] Grass, A.J., Structural features of turbulent flow over smooth and rough boundaries, *J. Fluid Mech.,* 50(2), 233–255, 1971.

[17] Hirata, M. and Kasagi, N., Studies of large-eddy structures in turbulent shear flows with the aid of flow visualization techniques, *Studies in Heat Transfer,* Hartnett J.P., et al., Eds., Hemisphere, 1979.

[18] Hussain, A.K.M.F., Coherent structures and turbulence, *J. Fluid Mech.,* 173, 303–356, 1986.

[19] Kasagi, N., Sumitani, Y., Suzuki, Y., and Iida, O., Kinematics of the quasi-coherent vortical structure in near-wall turbulence, *Int. J. Heat Fluid Flow,* 16, 2–10, 1995.

[20] Kline, S.J., Reynolds, W.G., Schraub, F.A., and Runstadler, P.W., The structure of turbulent boundary layers. *J. Fluid Mech.,* 30(4), 741–773, 1969.

[21] Kovasznay, L.S.D., Kibens, V., and Blackwelder, R.F., Large-scale motion in the intermittent region of a turbulent boundary layer, *J. Fluid Mech.,* 41, 283–325, 1970.

[22] Mankbadi, R.R., Dynamics and control of coherent structure in turbulent jets, *Appl. Mech. Rev.,* 45(6), 219–247, 1992.

[23] Miyake, Y., Ushiro, R., and Morikawa, T., On the regeneration of quasi-streamwise eddies, *Proc. Tenth Symp. Turbulent Shear Flows,* Penn State University, 1995.

[24] Offen, G.R. and Kline, S.J., Combined dye-streak and hydrogen-bubble visual observations of a turbulent boundary layer, *J. Fluid Mech.,* 62(2), 223–239, 1974.

[25] Robinson, S.K., The kinematics of turbulent boundary layer structure, *NASA Tech. Memorandum 103859,* 1991a.

[26] Robinson, S.K., Coherent motions in the turbulent boundary layer, *Ann. Rev. Fluid Mech.,* 23, 601–639, 1991b.

[27] Robinson, S.K., Kline, S.J. and Spalart, P.R., A review of quasi-coherent structures in a numerically simulated turbulent boundary layer, *NASA TM-102191,* 1989.

[28] Smith, C.R. and Metzler, S.P., The characteristics of low-speed streaks in the near-wall region of a turbulent boundary layer, *J. Fluid Mech.,* 129, 27–54, 1983.

[29] Spalart, P.R., Direct simulation of a turbulent boundary layer up to $Re_\theta = 1410$, *J. Fluid Mech.,* 187, 61–98, 1988.